

# Soft X-ray Induced Radiation Damage in Dip-and-Pull Photon Absorption and Photoelectron Emission Experiments

Shang-Hong Cheng, Chien-Hung Chang, Juan-Jesus Velasco-Velez, and Bo-Hong Liu\*

Cite This: *J. Phys. Chem. C* 2024, 128, 14381–14387

Read Online

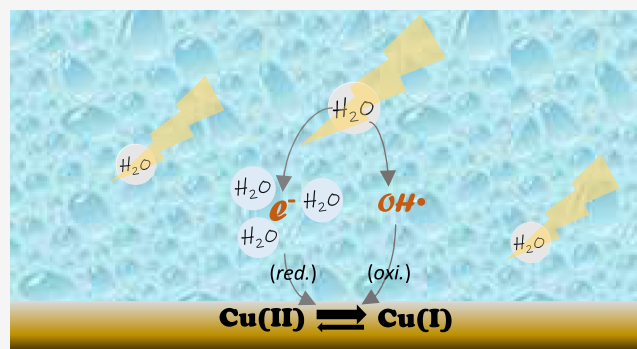
ACCESS |

Metrics & More

Article Recommendations

Supporting Information

**ABSTRACT:** X-ray irradiation can induce chemical reactions on surfaces. In X-ray spectroscopic experiments, such reactions may result in spectrum distortion and are termed radiation damage. In this study, we investigate the X-ray-induced chemical reaction at the partially oxidized copper surface in the settings of the dip-and-pull experiment, a method that generates liquid–solid interfaces for in situ X-ray photoelectron spectroscopy (XPS) studies. In dense water vapor resembling the predipping condition, a series of time-elapsing X-ray absorption spectra acquired in total electron yield mode (TEY-XAS) shows that X-ray exposure causes copper reduction, which follows first-order kinetics and occurs only at the surface shallower than the probing depth of TEY-XAS. At the solid–water interface created by the dip-and-pull method, the chemical reduction of surface copper is also identified by XPS. We conclude that the reduction is driven by the product of water radiolysis, where the reducing solvated electron prevails against the oxidizing OH radical and results in an overall reduction of surface copper ions.



## INTRODUCTION

Soft X-ray synchrotron radiation has been regularly used in spectroscopy experiments. X-ray absorption spectroscopy (XAS) excited with soft X-ray is advantageous over hard X-ray in several aspects.<sup>1</sup> It covers 3d transition metal's L-edge adsorption, which provides precise probing of covalency at transition metal sites. The energy resolution of L-edge X-ray absorption spectra is substantially higher than that of K-edge spectra because of the longer lifetime of 2p core holes and the better monochromator energy resolution at lower photon energies. In addition, soft X-ray reaches the K edge of carbon, nitrogen, and oxygen, which are major constituents of ligands and adsorbents. This allows for direct characterization of the molecules binding to the transition metals. Compared to hard X-ray, the lower penetration depth of soft X-ray photon results in a shallower information depth and, consequently, better surface sensitivity for the spectroscopy experiment.<sup>2</sup> On the other hand, the majority of synchrotron photoelectron spectroscopy (XPS) is done with soft X-ray also because of the superior beamline resolving power and the better surface sensitivity that results from shorter inelastic mean free path (IMFP) of low kinetic energy electron.

In situ soft X-ray XAS and XPS have been highly developed for the last decades and have become indispensable tools for studying electrochemical active interfaces.<sup>3,4</sup> Probing solid/ aqueous interfaces with photon/electron of limited IMFP requires sophisticated instrumentation.<sup>5</sup> A handful of designs based on working electrodes comprising a sample-loaded

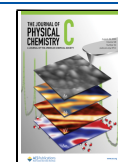
membrane have been reported. For in situ XAS, samples are loaded on a thin layer of X-ray transparent materials as the working electrode for setting up an electrochemical cell.<sup>6,7</sup> The XPS measurement is more challenging due to the limited IMFP of photoelectrons. One approach is to load the sample on a membrane of water-permeating material.<sup>8</sup> This way, the sample on the measuring side can be soaked with the electrolyte solution leaked from the back. Another method is depositing the sample on a double-layer graphene, supported on a Si<sub>3</sub>N<sub>4</sub> membrane etched with an array of through holes.<sup>9</sup> The double-layer graphene is thick enough to separate the electrolyte solution from the vacuum without blocking the photoelectrons. Dip-and-pull is another well-adopted approach.<sup>10</sup> As the name suggests, a solid–aqueous interface to be probed is created by dipping a dry electrode into an electrolyte-filled beaker, followed by a pull-out, which drags up a thin solution film a few tens of nanometers thick. According to the IMFP simulation, the electrochemical active interface behind the water meniscus can be studied efficiently with tender X-ray photoelectron spectroscopy.<sup>11</sup> However, a recent

Received: February 18, 2024

Revised: July 7, 2024

Accepted: July 12, 2024

Published: August 20, 2024



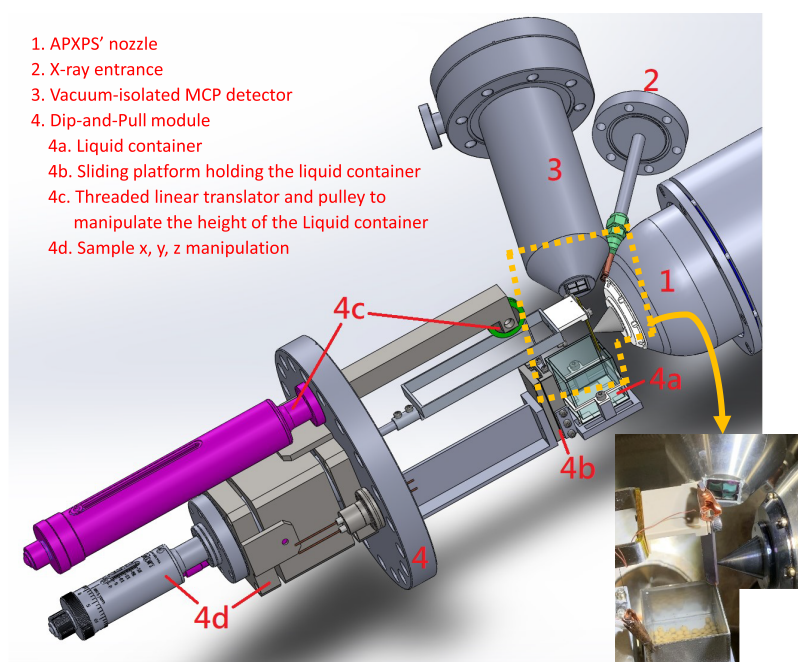


**Figure 1.** CAD drawing and photograph of the experimental setup. The chamber wall of the drawing is made invisible for clarity. The 8 in. flange houses essential dip-and-pull components—sample manipulation, beaker height adjustment, and electrical feedthroughs. The 4.5 in. port hosts an isolated MCP for fluorescence detection. The X-ray enters from the 2.75" port through a tubing, with a  $\text{Si}_3\text{N}_4$  membrane glued at the end. The cone is the APXPS nozzle, which is not used in this experiment.

study shows that soft X-ray can also be an appropriate excitation source for dip-and-pull-based XPS.<sup>12</sup>

The brilliance of synchrotron X-rays is an advantage for spectroscopy experiments; however, photon-induced sample damage is not uncommon. In conventional soft X-ray XAS and XPS experiments, the sample is kept under vacuum condition. Within the volume of penetration, a photon incident on a sample is absorbed. It may trigger successive processes, such as direct bond cleavage, photon-simulated desorption, and electron cascade that terminates with localized thermalization.<sup>13</sup> Some processes change the spectra, consequently complicating data interpretation.

In *in situ* experiments, the beam damaging effect becomes more ubiquitous, as the photon/photoelectron interacts not only with the sample but also with the molecules around the sample. The reaction scheme depends on the experimental configuration and varies from case to case. For instance, photon-induced electrolyte degradation was reported in an ambient-pressure XPS (APXPS) based *in situ* electrochemical experiment;<sup>14</sup> in another work that measures vanadium K-edge XAS, photon facilitates the reduction of supported vanadium oxide when the sample is placed in reducing gases, such as ethanol or hydrogen.<sup>15</sup> A flow-cell-based Cu  $L_3$ -edge XAS shows that copper oxide is oxidized during the spectrum acquisition in 0.1 M NaOH, but is reduced when methanol of 0.1 M is added in the flow liquid.<sup>16</sup> Since beam damage is common in *in situ* X-ray spectroscopic experiments, the scanning must be performed carefully to avoid such an experimental effect distorting the data. The knowledge of the specific experimental configurations helps the experimenter to identify the beam-induced effect and quickly develop a strategy to circumvent the issue during the experiment.

In this study, we track the chemical transformation of a copper surface under dip-and-pull-related experimental conditions and elucidate the origin of the transformation. In the

first part, we use XAS to investigate the collective effect of dense water vapor with the X-ray beam on the sample. This environment resembles the dip-and-pull experimental condition, in which the sample is at the position ready to be dipped into the electrolyte. In the second part, we used XPS to study the sample surface covered with a thin layer of electrolyte solution. This condition is created by dipping the sample into the electrolyte and then pulled out. In both cases, a beam-induced spectral change is recorded, and the driving reaction scheme is proposed.

## METHODS

The XAS experiment was performed at the Taiwan Light Source (TLS) beamline 24A APXPS endstation of the National Synchrotron Radiation Research Center, Taiwan.<sup>17</sup> We modularize the essential components of the dip-and-pull experiment on an 8" flange so that the endstation can be swiftly reconfigured for different types of experiments. As depicted in the drawing and the photograph in Figure 1, the module includes a sample manipulating set that allows the movement in *x*, *y*, and *z* directions, where the axial direction is manipulated by a linear motion feedthrough, and the other two are by a gimbal designed in-house. The liquid container is mounted on a vertical sliding platform maneuvered by a linear motion feedthrough through a thread over a pulley. The electrolyte solution level relative to the sample can be adjusted by lifting-descending the liquid container. Electrical feedthroughs for the drain current readout, temperature measurement, and electrochemical operations are included. A handful of zeolite is added to the liquid to slow down the outgassing and ease the bumping during the pumping down.

Unfortunately, the XPS experiment in dip-and-pull configuration is very limited at TLS 24A. Due to the low photon energy and insufficient flux, counts are too low to generate a quality spectrum in a reasonable time. Alternatively, we ran the

in situ experiment using XAS. The absorption signal is acquired with either total electron yield (TEY) or total fluorescent yield (TFY). The former is obtained by directly recording the sample drain current while energetically sweeping the X-ray photon through the adsorption edge. As for the TFY, the fluorescent photon is collected with a multichannel plate (MCP) detector. Since an operating MCP detector cannot be exposed to water vapor, we house it in a stainless steel container that is constantly pumped with a turbo molecular pump, leaving a  $\text{Si}_3\text{N}_4$  window photon passage pointing toward the sample. The  $\text{Si}_3\text{N}_4$  membrane is supported on four  $6.5 \times 6.5 \text{ mm}^2$  frames arranged in a  $2 \times 2$  grid. A  $200\text{-}\mu\text{m}$ -thick membrane ensures it withstands a few tens of mbars of pressure difference with fluctuations. Between 900 and 1000 eV, the photon flux at TLS 24A is around  $1 \times 10^{10}$  photons per second.<sup>18</sup> As for dip-and-pull APXPS, the experiment was conducted on the HIPPIE beamline's electrochemical endstation at MAX lab, Sweden.<sup>19</sup> All spectra were taken with a 1600 eV excitation energy. The photon flux is around  $1 \times 10^{12}$  photons per second.

The copper foil used for the dip-and-pull XAS experiment is of 99.999% purity and was purchased from Sigma-Aldrich. The specimen was tailored to a  $50 \text{ mm} \times 5 \text{ mm}$  strip to fit the setup. After scrubbing with sandpaper to expose the metallic surface, the sample was sonicated in an acetone bath, ethanol bath, and then DI water bath, each for 10 min. The oxidized copper layer was grown by heating the copper stripe to  $150 \text{ }^\circ\text{C}$  in an Ar-balanced 20%  $\text{O}_2$  for 15 min. As an exception, the XAS data in Figure 5 were acquired with the sample prepared with the above-mentioned condition but annealed in air. The sample for the dip-and-pull APXPS experiment is a 150 nm-thick copper film PVD-deposited on a Si(100) supported X-ray mirror capped with a rhodium layer. No trace of photoelectron from the elements underneath the copper can be detected in XPS. The surface was soaked in 20 mM of benzotriazole for 20 min to slow down the oxidation. The solution for the dip-and-pull experiment is 0.5 M NaCl aqueous solution.

## RESULTS AND DISCUSSION

Figure 2 shows Cu  $L_3$ -edge XAS from TEY (black) and TFY (red) of an oxidized copper surface. During the measurement, the chamber pressure is pumped down to  $1 \times 10^{-2}$  mbar after loading the sample in the atmosphere. In TEY-XAS, the spectrum features a main adsorption edge at 933.7 eV and a pre-edge peak at 931.3 eV. Compared to the Cu  $L_3$ -edge XAS reported in the literature,<sup>20,21</sup> the 933.7 eV adsorption edge with a sharp postedge drop is a feature of Cu(I), whereas the pre-edge peak at 931.3 eV signifies Cu(II), which comes from cupric oxide plus cupric hydroxide at the surface. The hump that starts rising from 936.4 eV and peak at 937.5 eV is minimal. This indicates that the TEY-XAS incorporates negligible metallic copper. The chemical state in TEY-XAS, therefore, consists of Cu(I) and Cu(II). The red curve in Figure 2 represents the XAS taken with TFY. Although self-absorption flattened the spectrum, the adsorption edge at 931.3 eV with postedge ripples features metallic copper. TEY-XAS with the soft-X-ray photon has a shallow probing depth of up to ten nanometers, whereas for TFY-XAS, atoms located hundreds of nm underneath the surface contribute to the spectrum because of the long penetration depth of the photon.<sup>22</sup> The contrast between the TEY-XAS and TFY-XAS in Figure 2 reveals that the sample consists mainly of a metallic

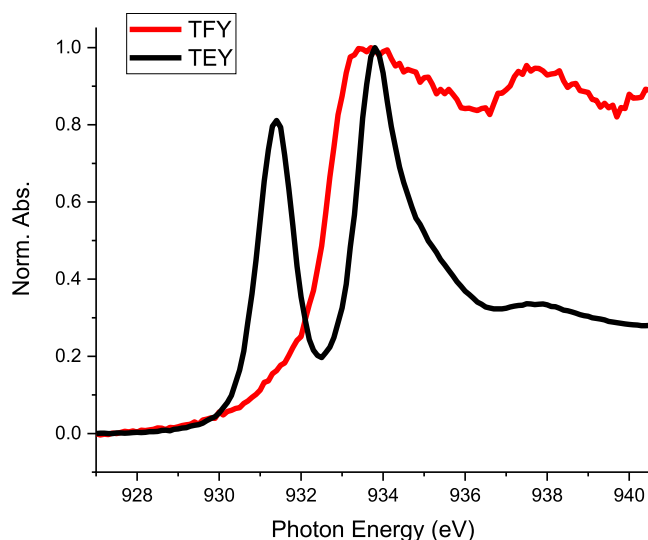


**Figure 2.** X-ray adsorption spectra of the oxidized copper measured in vacuum and recorded with total electron yield (TEY) and total fluorescent yield (TFY). In TEY-XAS, the pronounced pre-edge feature represents Cu(II), and the sharp decrease after the 933.7 eV main peak resembles Cu(I). In TFY-XAS, although severe self-absorption flattened the spectral feature, the postedge ripple of metallic copper can still be identified.

copper body covered with a mixed Cu(I)/Cu(II) layer, whose thickness is presumably less than ten nanometers.

In the dip-and-pull experiment, the background pressure is governed by the vapor pressure of the electrolyte solution. Because of the vaporization cooling, the solution temperature during the experiment was below room temperature. In the present experiment, the equilibrium temperature is around  $15 \text{ }^\circ\text{C}$ . As a result, the chamber's lowest reachable pressure is around 13 mbar. This level of background pressure scatters the photon/electron considerably; therefore, only XAS experiments can be effectively carried out at TLS 24A.

Figure 3 shows the TEY of Cu  $L_3$ -edge XAS taken consecutively over time in 13 mbar of water vapor. To highlight the evolving trend, the spectra are aligned by leveling the baseline and overlapping the pre-edge background and then normalizing to the summit of the main edge at 933.7 eV. One can see that the pre-edge at 931.3 eV shrinks continuously. The intensity ratio of the 931.3 eV peak to the 933.7 eV peak falls from 0.72 to 0.44 within 1.5 h. This indicates that the concentration of Cu(II) compared to Cu(I) drops, suggesting a chemical reduction. Since there is no obvious rise from 936.4 eV, the presence of metallic copper can be excluded. As a reference, in the TFY-XAS shown in Figure S1, the spectrum before and after the 90 min X-ray exposure in water does not show any change as expected.

Humidity tends to induce surface corrosion.<sup>23</sup> In the dip-and-pull experiment, all gases except water vapor are removed from the chamber during the pumping down. Before the sample was dipped into the solution, the surface is exposed to dense water vapor. In the present experimental condition, the equilibrium water vapor pressure is 13 mbar, while the sample temperature is  $20 \text{ }^\circ\text{C}$ . Although the relative humidity at the surface is around 60%, much lower than the dew point, a hydrophilic oxide/hydroxide surface could adsorb plenty of water. We have noticed that recently, Lee et al. discovered that hydrogen peroxide spontaneously forms in micrometer-sized

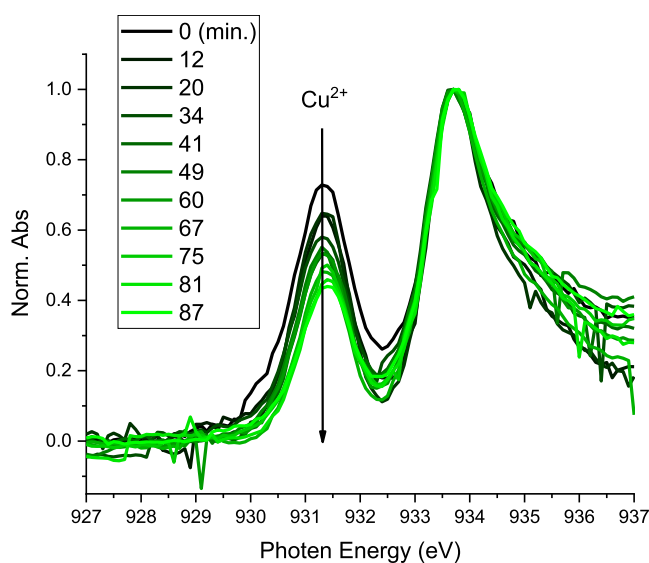


**Figure 3.** Cu  $L_3$ -edge TEY-XAS was taken repeatedly in 13 mbar water vapor. All spectra are offset, and the slope was adjusted to align their pre-edge background between 925 and 927 eV and normalized to the main edge at the 932 eV peak. A reduction of the pre-edge feature over time indicates the loss of Cu(II).

water droplets generated by nebulizing bulk water.<sup>24</sup> A few follow-up studies demonstrated that nebulization is not a prerequisite; instead, condensing microdroplets on a surface from the moisture also introduces  $H_2O_2$ , whose concentration depends on the hydrophilicity of the substrate and relative humidity and generally falls in the ppm range.<sup>25</sup> Knowing that  $H_2O_2$  is chemically active and can drive either oxidation or reduction,<sup>26</sup> we postulate that  $H_2O_2$  from the condensed water droplets may cause copper reduction observed in this humid environment.

To eliminate the possible effect from the X-ray, we expose the sample to the same 13 mbar of water vapor for 1.5 h and only turn on the X-ray for the XAS measurement before and after the water-vapor exposure. As shown in Figure S2a, the TEY-XAS of Cu  $L_3$  edge XAS before and after the exposure overlaps quite well. This indicates that the dense water vapor or the subsequent condensed water droplet/film does not induce the chemical transformation seen in Figure 3. In another control experiment, we inspect the sample irradiated by X-ray for 90 min in vacuum. Operationally, we scanned the Cu  $L_3$ -edge XAS repeatedly for 90 min and plotted only the first and last spectra, as shown in Figure S2b. The two identical spectra indicate that X-ray alone does not induce the reduction. The radiation effect occurs only in a humid environment, which resembles the “pre-dipping” condition in the dip-and-pull experiment.

Radiolysis of water was discovered more than a century ago. It has been studied comprehensively because of its profound impact.<sup>27</sup> The reaction scenario depends on the type of radiation that is involved. Soft X-ray belongs to the low-linear energy transfer (low LET) radiation, which refers to the radiation that does not hold charge or mass. In the low-LET induced water radiolysis, the initial chemical product contains highly reactive radical species, including hydroxyl radical, hydrogen radical, and hydrated electrons.<sup>28</sup> Hydroxyl radicals are strong oxidative species. It was reported that the reaction  $Cu(I) + \cdot OH \rightarrow Cu(II) + OH^-$  taking place in an aqueous environment has a rate constant of  $2 \times 10^{10}$ .<sup>28</sup> On the contrary,

atomic hydrogen and hydrated electrons are reducing agents. The rate constant for the Cu(II) reducing reactions in aqueous solution is  $9.1 \times 10^7$  for  $\cdot H + Cu^{2+} \rightarrow H^+ + Cu^+$  and  $3.3 \times 10^{10}$  for  $e^- + Cu^{2+} \rightarrow Cu^+$ . The hydroxyl radical oxidation and the hydrated electron reduction have about the same rate constant and an opposite reactant/product pair, whereas the rate constant for the atomic-hydrogen reduction is negligible compared with the other two. The actual rate constant may vary from condition to condition. From the TEY-XAS spectra in Figure 3, overall, the reduction prevails in the predipping condition of the dip-and-pull experiment. As the reduction and the oxidation reactions are both first-order, the kinetics can be described with an exponential equation, as derived on page S3 of the Supporting Information.

In Figure 4, the  $I_{931.3 \text{ eV}}$  to  $I_{933.7 \text{ eV}}$  ratio is plotted with respect to the time elapsed. Exponential fitting results in a

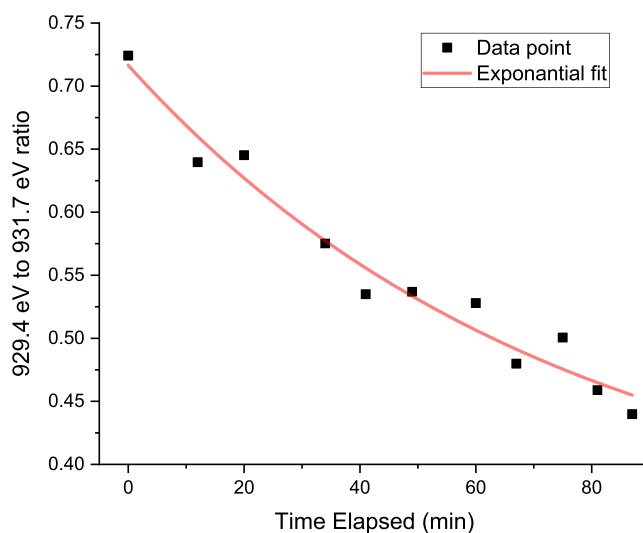


**Figure 4.** Exponential fitting to the 931.3, 933.7 eV peak-to-peak ratio with respect to the irradiation time. The data points and the fitting parameters are shown in the Tables S1 and S2, respectively, of the Supporting Information.

favorable  $R$ -squared value of 0.964, suggesting that the reaction follows the scenario described above. The fitted trend converges at  $y_0 = 0.337$ , indicating that even if the irradiation in water vapor lasts for a very long period of time, a significant amount of Cu(II) will remain. A likely explanation is that the TEY-XAS probes deeper than the region where the surface reduction takes place. The remaining Cu(II) in the spectrum comes from the volume buried deep enough under the surface to not be affected by the gas phase reactants.

Water radiolysis may depend on the photon energy. To examine the conclusion drawn so far, we perform the X-ray exposure treatment in water vapor using different X-ray photon energies. As the absorbance may influence the water radiolysis yield, we chose two different photon energies at the opposite side of the oxygen K-edge: 450 and 600 eV. At TLS 24A, these two photon energies are monochromated by an 800 l/mm grating, which results in roughly an order of magnitude higher photon flux than the 1600 l/mm grating used to produce the photon of energy around the Cu  $L_3$ -edge. Figure 5a shows how 450 eV photons affect the copper surface oxidation state in water vapor: the Cu(II) intensity drops to a moderate extent. This shows that even though the photon energy shifts away from the copper absorption edge, the spectrum varies in the

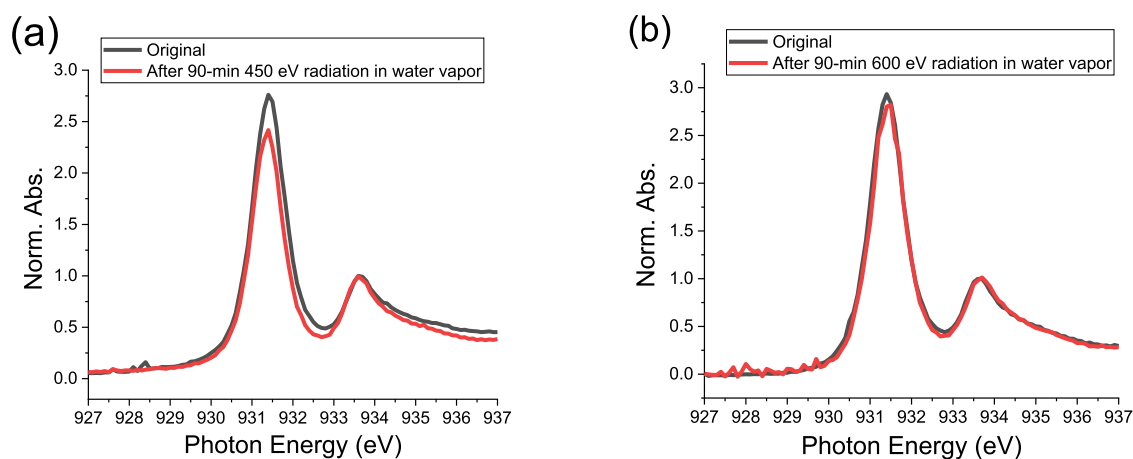


**Figure 5.** Cu  $L_3$ -edge TEY-XAS before and after a 90 min X-ray exposure by (a) 450 eV and (b) 600 eV photon. The chamber is filled with 13-mbar water vapor during the radiation exposure as well as the XAS scans.

same way. This rules out the doubt that the electronically excited surface copper, in some ways, causes the reduction. Notice that even though the photon flux is approximately 1 order of magnitude higher than  $\sim 930$  eV, the copper reduction is milder. This is attributed to the lower penetrating power of the softer photon. In Figure 5b, the photon energy to induce water radiolysis is 600 eV. The reduction can barely be identified. It seems that the water vapor between the beam entrance and the sample blocks most of the photons, and the reduction of copper is therefore suppressed.

We further used APXPS to investigate the influence of water radiolysis on a copper sample in the dip-and-pull experimental condition. The experiment was performed at the MAX IV HIPPIE beamline's APXPS-2 endstation, a station dedicated to electrochemical experiments. The copper-deposited sample was coated with a BTA layer by soaking in 20 mM BTA solution. This is to protect the surface from ambient oxidation. As shown in the time-elapsed N 1s spectra in Figure S3, the signal almost disappears instantaneously upon X-ray irradiation, suggesting that the BTA layer decomposes.

Figure 6a shows the O 1s spectra from liquid-water-covered copper generated by the dip-and-pull method. To track the effect of water radiolysis on the surface, we record the spectra consecutively with the analyzer running in the snapshot mode. With the pass energy set to 200 eV, the spectral window has a 20 eV span, which covers the entire O 1s spectrum, including the signal from the gas phase. Ten seconds of counting time for each frame results in an acceptable signal-to-noise ratio. The three components at 534.5, 531.9, and 529.6 eV represent gas-phase water, liquid-phase water plus hydroxyls, and surface oxides, respectively. The simultaneous appearance of the gas, liquid, and solid phases in a single spectrum suggests that the spectroscopic probe reaches the solid/liquid interface. In the spectra, the peak area from the liquid water/hydroxyl and the oxide changes over time: the count from surface oxide drops, whereas the signal from liquid water/hydroxyl enhances. Figure 6b summarizes the integrated counts and their evolution trends. The liquid water/hydroxyl counts increase fast at the beginning and slow down over time, whereas for the oxide peak, the count drops roughly at the same pace until the peak dyes out. The fact that the intensity of the liquid water/hydroxyl peak and the oxide peak do not evolve at the same pace implies that different forces drive the changes. The loss of oxide oxygen indicates surface reduction. As previously

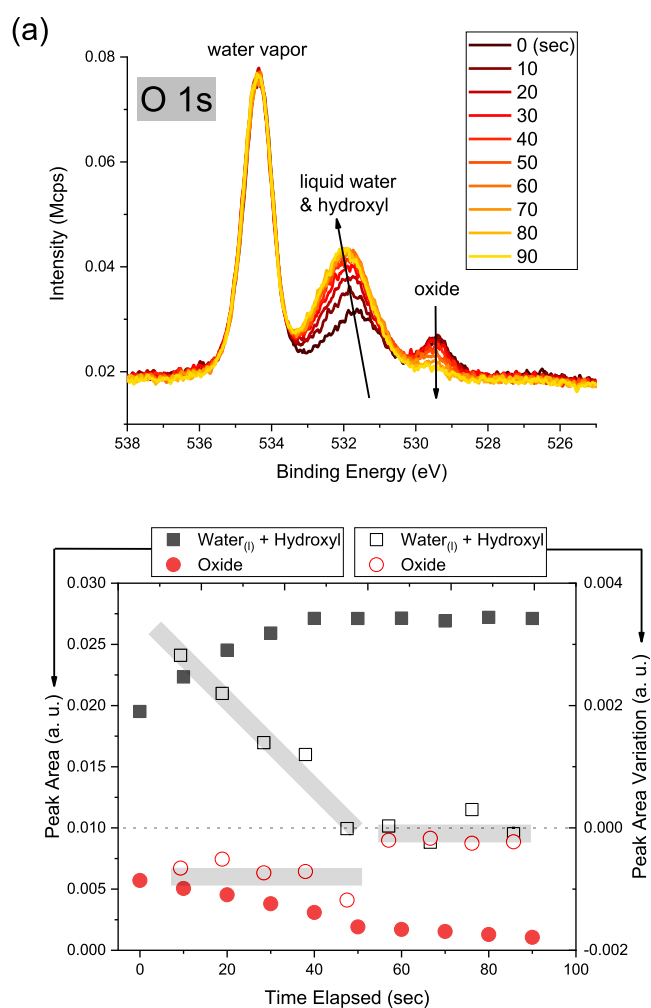


**Figure 6.** (a) XPS of the O 1s from a copper/water interface generated by the dip-and-pull method. The measurement used the spectrometer's snapshot mode to trade the energy resolution for time resolution. Each spectrum counts for 10 s. (b) Fitted peak area of oxide and liquid water plus hydroxyl are plotted in solid data points. The difference between two adjacent peak areas is plotted in a hollow data point, showing the evolving trends, which are highlighted with gray strips.

discussed, when performing XAS in a humid environment, water radiolysis reduces surface copper. As the photon flux and water density exceed in the present case, the water radiolysis is more ferocious and is likely to be the driving force for the surface reduction. On the other hand, the growth of liquid water/hydroxyl may come from the accumulation of liquid water on the surface. As the spectral resolution from the snapshot mode is compromised, the liquid water and hydroxyl components merge into a single spectral envelope and are hard to distinguish accurately. However, it is obvious that the summit of the envelope shifts to higher binding energy as the peak grows larger. This suggests that the growth is likely due to the increase of liquid water, whose O 1s BE is around 533 eV, rather than hydroxyl at around 531 eV.<sup>29</sup> We postulate that the gain of liquid water is caused by an increase in the surface hydrophilicity. Although the surface BTA layer protects the surface from being oxidized to an extent, it modifies the surface property, including turning the surface hydrophobic.<sup>30</sup> When the BTA layer is scavenged by the reactive product of the water radiolysis, as depicted by the N 1s spectra in Figure S3, the intrinsic hydrophilicity of the oxide layer is resumed, resulting in a growing liquid water layer seen in the O 1s spectra.

Noticed that our experimental condition is somewhat comparable with Weatherup and co-workers' work,<sup>16</sup> in which the beam-damaging effect on a copper surface in a flow-cell-based XAS experiment is reported. The work concludes that in 0.1 M NaOH aqueous solution, the 931 eV peak of the Cu L<sub>3</sub>-edge is enhanced during the XAS scans. The authors account for the enhancement of surface oxidation. Seemingly, this conclusion contradicts our finding; however, we think that the basic environment and the liquid flow in Weatherup and co-workers' experiment may affect the surface composition. In the literature, copper oxide dissolution in an alkaline solution has been reported.<sup>31,32</sup> One could expect OH to facilitate the dissolution of surface copper oxides, which may then be removed from the surface by the liquid flow. The differential of the surface Cu(I) and Cu(II) removing rate may be what causes the change in the spectrum. This may explain the opposite conclusion from Weatherup and co-workers' study and the presented work. Moreover, in the reaction scheme proposed in the presented work, oxidation and reduction take place simultaneously and are primarily induced by OH radicals and hydrated electrons, respectively. This echoes Weatherup and co-worker's finding, which shows that when adding methanol, an OH radical scavenger, the oxidation is suppressed and results in a pronounced surface reduction.

## CONCLUSIONS

We investigated the soft X-ray-induced copper surface reaction in water-rich environments that resembles the dip-and-pull experimental conditions. With soft X-ray irradiation in 13 mbar of water vapor evaporated from the liquid container placed in the vacuum chamber, TEY-XAS revealed that Cu(II) of a partially oxidized copper surface is reduced to Cu(I). Kinetic analysis shows that the reduction follows first-order kinetics and involves only the atoms at the shallow surface. In the case of a thin liquid water meniscus covering the copper surface, the loss of surface oxide is identified with XPS, indicating a surface chemical reduction. We attribute the reduction to the product of water radiolysis, where the reducing solvated electron prevails over the oxidizing OH radical.

## ASSOCIATED CONTENT

### Supporting Information

The Supporting Information is available free of charge at <https://pubs.acs.org/doi/10.1021/acs.jpcc.4c01067>.

TFY-XAS spectra of the partially oxidized copper foil before and after X-ray the exposure to water vapor, derivation of the data-fitting equation, TFY-XAS spectra before and after either X-ray exposure or water vapor exposure, data points and the fitted parameters of the regression analysis, and N 1s XPS spectra showing the beam-induced BTA degradation (PDF)

## AUTHOR INFORMATION

### Corresponding Author

**Bo-Hong Liu** – Scientific Research Division, National Synchrotron Radiation Research Center, 300092 Hsinchu, Taiwan; Chemical Science Division, Lawrence Berkeley National Laboratory, Berkeley, California 94720, United States; [orcid.org/0000-0001-7347-7633](https://orcid.org/0000-0001-7347-7633); Email: [Liu.bh@nsrc.org.tw](mailto:Liu.bh@nsrc.org.tw)

### Authors

**Shang-Hong Cheng** – Scientific Research Division, National Synchrotron Radiation Research Center, 300092 Hsinchu, Taiwan

**Chien-Hung Chang** – Experimental Facility Division, National Synchrotron Radiation Research Center, 300092 Hsinchu, Taiwan

**Juan-Jesus Velasco-Velez** – Department of Heterogeneous Reactions, Max Planck Institute for Chemical Energy Conversion, 45470 Mülheim an der Ruhr, Germany; Experiments Division, ALBA Synchrotron Light Source, Cerdanyola del Vallés, Barcelona 08290, Spain; [orcid.org/0000-0002-6595-0168](https://orcid.org/0000-0002-6595-0168)

Complete contact information is available at: <https://pubs.acs.org/doi/10.1021/acs.jpcc.4c01067>

### Notes

The authors declare no competing financial interest.

## ACKNOWLEDGMENTS

B.H.L., S.H.C., and C.C.C. thank Dr. Yaw-Wen Yang for his advice on the dip-and-pull module instrumentation and Dr. Zong-Ren Yang for assisting with the experiment. They also thank Dr. Wu Tai-Hsin, Dr. Ying-Rui Lu, and Dr. Lo-Yueh Chang for discussing the XAS data. The XAS part of the work is supported by the National Synchrotron Radiation Research Center, Taiwan. B.H.L. and J.J.V.V. thank Mr. Suyun Zhu, Dr. Mattia Scardamaglia, and Dr. Andrey Shavorskiy for their full support on the APXPS experiment performed at the HIPPIE beamline at MaxLab, Sweden. They also thank Dr. Hendrik Bluhm, Dr. Slavomir Némšák, and Dr. Miquel Salmeron for their help in planning the APXPS experiment for the beamtime at HIPPIE. The expense for carrying out the APXPS experiment was funded by the Office of Basic Energy Sciences (BES) of the U.S. Department of Energy (DOE) under Contract No. DE-AC02-05CH11231, through the Structure and Dynamics of Materials Interfaces program (FWP KC31SM).

## REFERENCES

- (1) Baker, M. L.; Mara, M. W.; Yan, J. J.; Hodgson, K. O.; Hedman, B.; Solomon, E. I. K- and L-edge X-ray absorption spectroscopy (XAS) and resonant inelastic X-ray scattering (RIXS) determination of coordinational orbital covalency (DOC) of transition metal sites. *Coordination chemistry reviews* **2017**, *345*, 182–208.
- (2) Knop-Gericke, A.; Groot, F. M. F. D.; Bokhoven, J. A. V.; Ressler, T.; Soft X-ray Absorption Methods. In *In-Situ Spectroscopy of Catalysts*, Nalwa, H. S., Ed. American Scientific Publishers, 2004.
- (3) Crumlin, E. J.; Bluhm, H.; Liu, Z. In situ investigation of electrochemical devices using ambient pressure photoelectron spectroscopy. *J. Electron Spectrosc. Relat. Phenom.* **2013**, *190*, 84–92.
- (4) Jiang, P.; Chen, J.-L.; Borondics, F.; Glans, P.-A.; West, M. W.; Chang, C.-L.; Salmeron, M.; Guo, J. In situ soft X-ray absorption spectroscopy investigation of electrochemical corrosion of copper in aqueous NaHCO<sub>3</sub> solution. *Electrochem. Commun.* **2010**, *12* (6), 820–822.
- (5) Carbonio, E. A.; Velasco-Velez, J.-J.; Schlögl, R.; Knop-Gericke, A. Perspective—Outlook on Operando Photoelectron and Absorption Spectroscopy to Probe Catalysts at the Solid-Liquid Electrochemical Interface. *J. Electrochem. Soc.* **2020**, *167* (5), No. 054509.
- (6) Villullas, H. M.; Ometto, F. B.; Alvarenga, G. M.; Vicentin, F. C. A novel electrochemical cell for operando X-ray absorption measurements at low energies: Probing electrochemically induced electronic changes in palladium. *Electrochemistry communications* **2018**, *94*, 14–17.
- (7) Velasco-Velez, J.-J.; Wu, C. H.; Pascal, T. A.; Wan, L. F.; Guo, J.; Prendergast, D.; Salmeron, M. The structure of interfacial water on gold electrodes studied by x-ray absorption spectroscopy. *Science* **2014**, *346* (6211), 831–834.
- (8) Pfeifer, V.; Jones, T. E.; Vélez, J. J. V.; Arrigo, R.; Piccinin, S.; Hävecker, M.; Knop-Gericke, A.; Schlögl, R. In situ observation of reactive oxygen species forming on oxygen-evolving iridium surfaces. *Chem. Sci.* **2017**, *8* (3), 2143–2149.
- (9) Velasco-Velez, J. J.; Pfeifer, V.; Hävecker, M.; Weatherup, R. S.; Arrigo, R.; Chuang, C. H.; Stotz, E.; Weinberg, G.; Salmeron, M.; Schlögl, R. Photoelectron spectroscopy at the graphene–liquid interface reveals the electronic structure of an electrodeposited cobalt/graphene electrocatalyst. *Angew. Chem., Int. Ed.* **2015**, *54* (48), 14554–14558.
- (10) Karslioglu, O.; Nemšák, S.; Zegkinoglou, I.; Shavorskiy, A.; Hartl, M.; Salmassi, F.; Gullikson, E. M.; Ng, M. L.; Rameshan, C.; Rude, B.; et al. Aqueous solution/metal interfaces investigated in operando by photoelectron spectroscopy. *Faraday Discuss.* **2015**, *180*, 35–53.
- (11) Axnanda, S.; Crumlin, E. J.; Mao, B. H.; Rani, S.; Chang, R.; Karlsson, P. G.; Edwards, M. O. M.; Lundqvist, M.; Moberg, R.; Ross, P. Using “Tender” X-ray Ambient Pressure X-Ray Photoelectron Spectroscopy as A Direct Probe of Solid-Liquid Interface. *Sci. Rep.* **2015**, *5*, 9788.
- (12) Kallquist, I.; Lindgren, F.; Lee, M.-T.; Shavorskiy, A.; Edstrom, K.; Rensmo, H.; Nyholm, L.; Maibach, J.; Hahlin, M. Probing Electrochemical Potential Differences over the Solid/Liquid Interface in Li-Ion Battery Model Systems. *ACS Appl. Mater. Interfaces* **2021**, *13* (28), 32989–32996.
- (13) Thomas, III, J. H.; Photon Beam Damage and Charging at Solid Surfaces. In *Beam Effects, Surface Topography, and Depth Profiling in Surface Analysis*, Czanderna, A. W.; Madey, T. E.; Powell, C. J., Eds. Plenum Press: New York, 1998.
- (14) Arble, C.; Guo, H.; Strelcov, E.; Hoskins, B.; Zeller, P.; Amati, M.; Gregoratti, L.; Kolmakov, A. Radiation damage of liquid electrolyte during focused X-ray beam photoelectron spectroscopy. *Surf. Sci.* **2020**, *697*, No. 121608.
- (15) Zabilska, A.; Clark, A. H.; Ferri, D.; Nachtgeal, M.; Kröcher, O.; Safonova, O. V. Beware of beam damage under reaction conditions: X-ray induced photochemical reduction of supported VOx catalysts during in situ XAS experiments. *Phys. Chem. Chem. Phys.* **2022**, *24*, 21916–21926.
- (16) Weatherup, R. S.; Wu, C. H.; Escudero, C.; Pérez-Dieste, V.; Salmeron, M. B. Environment-dependent radiation damage in atmospheric pressure X-ray spectroscopy. *J. Phys. Chem. B* **2018**, *122* (2), 737–744.
- (17) Wang, C.-H.; Liu, B.-H.; Yang, Y.-W. Ambient Pressure X-Ray Photoelectron Spectroscopy (APXPS): Present Status and Future Development at NSRRC. *Synchrotron Radiation News* **2022**, *35* (3), 48–53.
- (18) Taiwan Light Source beamline 24A webpage. [https://tlns.nsrcc.org.tw/bd\\_page.aspx?lang=en&port=24A1&pid=1386](https://tlns.nsrcc.org.tw/bd_page.aspx?lang=en&port=24A1&pid=1386). (May 13th, 2024).
- (19) Zhu, S.; Scardamaglia, M.; Kundsén, J.; Sankari, R.; Tarawneh, H.; Temperton, R.; Pickworth, L.; Cavalca, F.; Wang, C.; Tissot, H. HIPPIE: a new platform for ambient-pressure X-ray photoelectron spectroscopy at the MAX IV Laboratory. *J. Synchrotron Radiat.* **2021**, *28* (2), 624–636.
- (20) Jiang, P.; Prendergast, D.; Borondics, F.; Porsgaard, S.; Giovanetti, L.; Pach, E.; Newberg, J.; Bluhm, H.; Besenbacher, F.; Salmeron, M. Experimental and theoretical investigation of the electronic structure of Cu<sub>2</sub>O and CuO thin films on Cu (110) using x-ray photoelectron and absorption spectroscopy. *J. Chem. Phys.* **2013**, *138* (2), No. 024704.
- (21) Hollmark, H.; Keech, P.; Vegelius, J.; Werme, L.; Duda, L.-C. X-ray absorption spectroscopy of electrochemically oxidized Cu exposed to Na<sub>2</sub>S. *Corros. Sci.* **2012**, *54*, 85–89.
- (22) de Groot, F.; Kotani, A. *Core Level Spectroscopy of Solids*. CRC Press, 2008.
- (23) FitzGerald, K.; Nairn, J.; Skennerton, G.; Atrens, A. Atmospheric corrosion of copper and the colour, structure and composition of natural patinas on copper. *Corros. Sci.* **2006**, *48* (9), 2480–2509.
- (24) Lee, J. K.; Walker, K. L.; Han, H. S.; Kang, J.; Prinz, F. B.; Waymouth, R. M.; Nam, H. G.; Zare, R. N. Spontaneous generation of hydrogen peroxide from aqueous microdroplets. *Proc. Natl. Acad. Sci. U. S. A.* **2019**, *116* (39), 19294–19298.
- (25) Lee, J. K.; Han, H. S.; Chaikasetsin, S.; Marron, D. P.; Waymouth, R. M.; Prinz, F. B.; Zare, R. N. Condensing water vapor to droplets generates hydrogen peroxide. *Proc. Natl. Acad. Sci. U. S. A.* **2020**, *117* (49), 30934–30941.
- (26) Bancroft, W. D.; Murphy, N. F. Oxidation and reduction with hydrogen peroxide. *J. Phys. Chem.* **1935**, *39* (3), 377–398.
- (27) Jonah, C. D. A short history of the radiation chemistry of water. *Radiation research* **1995**, *144* (2), 141–147.
- (28) Buxton, G. V.; Greenstock, C. L.; Helman, W. P.; Ross, A. B. Critical Review of rate constants for reactions of hydrated electrons, hydrogen atoms and hydroxyl radicals ( $\cdot$ OH/ $\cdot$ O<sup>-</sup> in Aqueous Solution. *Journal of physical and chemical reference data* **1988**, *17* (2), 513–886.
- (29) Trotochaud, L.; Head, A. R.; Pletincx, S.; Karslioglu, O.; Yu, Y.; Waldner, A.; Kyhl, L.; Hauffman, T.; Terry, H.; Eichhorn, B.; et al. Water Adsorption and Dissociation on Polycrystalline Copper Oxides: Effects of Environmental Contamination and Experimental Protocol. *J. Phys. Chem. B* **2018**, *122* (2), 1000–1008.
- (30) Cho, B.-J.; Shima, S.; Hamada, S.; Park, J.-G. Investigation of cu-BTA complex formation during Cu chemical mechanical planarization process. *Appl. Surf. Sci.* **2016**, *384*, 505–510.
- (31) Navarro, M.; May, P. M.; Hefter, G.; Königsberger, E. Solubility of CuO (s) in highly alkaline solutions. *Hydrometallurgy* **2014**, *147*, 68–72.
- (32) Palmer, D. A. Solubility measurements of crystalline Cu<sub>2</sub>O in aqueous solution as a function of temperature and pH. *Journal of solution chemistry* **2011**, *40* (6), 1067–1093.